

Temperature-filling Phase Diagrams for the 2D Hubbard-Holstein Model via Renormalized Migdal-Eliashberg Theory

Asadullah Bhuiyan and Frank Marsiglio

*Department of Physics and Theoretical Physics Institute,
University of Alberta, Edmonton, Alberta T6G 2E1, Canada*

(Dated: August 11, 2021)

Abstract.

I. INTRODUCTION: BARE HOLSTEIN MODEL

The model under consideration is the Holstein (or molecular crystal) model with Hamiltonian:

$$H = - \sum_{\langle ij \rangle} \sum_{\sigma} t_{ij} (c_{i\sigma}^{\dagger} c_{j\sigma} + c_{j\sigma}^{\dagger} c_{i\sigma}) - \mu \sum_{i\sigma} n_{i\sigma} + \sum_i \left(\frac{p_i^2}{2M} + \frac{1}{2} K x_i^2 \right) - \alpha \sum_{i\sigma} x_i n_{i\sigma} \quad (1)$$

where x_i and p_i are scalar position and momentum operators for the ion with mass M and spring constant K ($= M\omega_E^2$) at site i . $c_{i\sigma}^{\dagger}$ is the creation operator for an electron with spin σ at site i . Hopping occurs via the first term in the Hamiltonian, with probability amplitude t_{ij} . The chemical potential, μ , is chosen to give a set number density of electrons, n . The last term couples the electron density $n_{i\sigma} \equiv c_{i\sigma}^{\dagger} c_{i\sigma}$ with the lattice displacement, x_i at site i , with coupling constant α .

The ion momentum p_i , and displacement x_i are quantized in the usual way via (we set $\hbar \equiv 1$)

$$\begin{aligned} x_i &\equiv \sqrt{\frac{1}{2M\omega_E}} (a_i^{\dagger} + a_i) \\ p_i &\equiv i\sqrt{\frac{M\omega_E}{2}} (a_i^{\dagger} - a_i), \end{aligned} \quad (2)$$

where a_i^{\dagger} (a_i) creates (annihilates) a phonon at site i . Then Eq. (1) becomes

$$\begin{aligned} H &= -t \sum_{i,\delta} (c_{i\sigma}^{\dagger} c_{i+\delta\sigma} + c_{i+\delta\sigma}^{\dagger} c_{i\sigma}) - g\omega_E \sum_{i,\sigma} n_{i\sigma} (a_i + a_i^{\dagger}) \\ &+ \omega_E \sum_i a_i^{\dagger} a_i. \end{aligned} \quad (3)$$

The sum over i is over all sites in the lattice, whereas the sum over δ is over nearest neighbours. As the notation already suggests, we confine ourselves to nearest neighbour hopping only. In fact, for a given i , δ will be summed over nearest neighbours in the positive direction only (e.g. $+\hat{x}$ and $+\hat{y}$ in two dimensions), to avoid double counting.

The parameters in Eq. (3) are the hopping integral t , the phonon frequency ω_E , and the coupling of the electron to the oscillator degrees of freedom, $g\omega_E \equiv \alpha/\sqrt{2M\omega_E}$. Here g is the dimensionless coupling constant often used in the polaron literature² while $\lambda \equiv 2g^2(\omega_E/W)$ is the dimensionless parameter often used in the many-electron literature. In Refs. [1]

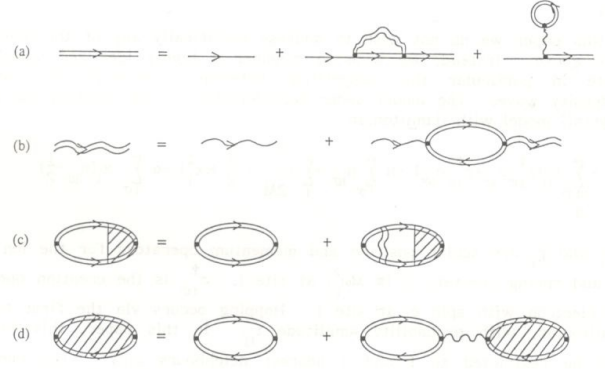


FIG. 1. Fully self-consistent equations for (a) the interacting electron propagator (straight double lines), (b), the interacting phonon propagator (wavy double line), (c) the singlet pairing susceptibility in the “ladder” approximation, and (d) the CDW susceptibility in the “bubble” approximation. Single lines represent non-interacting propagators.

and [2] we used $\lambda_0 \equiv \alpha^2/(M\omega_E^2)$, which clearly is related to λ via $\lambda \equiv \lambda_0/W$. For this reason, values of $\lambda_0 = 2t$ used in those studies correspond to $\lambda = 0.25$ (for a two-dimensional model with $W = 8t$). We will give a literature review later. Early references for the two-dimensional model are Scalettar et al.,³ Levine and Su⁴ and the author.¹ See also Noack et. al.³

A. Theoretical Details

To proceed with perturbation theory we transform Eq. (3) to reciprocal space. Using

$$c_{i\sigma}^{\dagger} \equiv \frac{1}{\sqrt{N}} \sum_{\vec{k}} e^{-i\vec{k}\cdot\vec{R}_i} c_{k\sigma}^{\dagger}, \quad (4)$$

$$c_{i\sigma} \equiv \frac{1}{\sqrt{N}} \sum_{\vec{k}} e^{+i\vec{k}\cdot\vec{R}_i} c_{k\sigma}, \quad (5)$$

$$a_i \equiv \frac{1}{\sqrt{N}} \sum_{\vec{q}} e^{+i\vec{q}\cdot\vec{R}_i} a_{\vec{q}}, \quad (6)$$

$$a_i^{\dagger} \equiv \frac{1}{\sqrt{N}} \sum_{\vec{q}} e^{-i\vec{q}\cdot\vec{R}_i} a_{\vec{q}}^{\dagger}, \quad (7)$$

Eq. (3) becomes

$$H = \sum_{\vec{k}, \sigma} (\epsilon_k - \mu) c_{k\sigma}^\dagger c_{k\sigma} + \omega_E \sum_q a_q^\dagger a_q - \frac{g\omega_E}{\sqrt{N}} \sum_{\vec{k}, \vec{q}} c_{k+q\sigma}^\dagger c_{k\sigma} (a_q + a_{-q}^\dagger), \quad (8)$$

where $\epsilon_k = -2t[\cos(k_x a) + \cos(k_y a)]$, with $k_x a = 2\pi n_1/N$ and $k_y a = 2\pi n_2/N$, with $-N/2 < n_i \leq N/2$ for $i = 1, 2$. Hereafter we set $a \equiv 1$. The perturbative approach is summarized diagrammatically in Fig. 1. The one-electron Green's function is given by

$$G(\vec{k}, i\omega_m) = [i\omega_m - (\epsilon_k - \mu) - \Sigma(\vec{k}, i\omega_m)]^{-1} \quad (9)$$

where $i\omega_m \equiv i\pi T(2m - 1)$ are the fermion Matsubara frequencies, and ϵ_k is the single particle energy obtained from diagonalizing the first term in the Hamiltonian (1). The index m takes on all integer values. The electron self-energy due to the electron-phonon interaction is given by $\Sigma(\vec{k}, i\omega_m)$. Similarly the phonon propagator is given by

$$D(\vec{q}, i\nu_n) = \frac{-2\omega_E}{(\omega_E^2 + \nu_n^2) + 2\omega_E \Pi(\vec{q}, i\nu_n)} \quad (10)$$

where $i\nu_n \equiv 2i\pi Tn$ are the boson Matsubara frequencies, and ω_E is the Einstein phonon frequency. The index n again takes on all integer values. In this model, because we have used a site-diagonal coupling, the unperturbed phonon frequency has no dispersion. Finally $\Pi(\vec{q}, i\nu_n)$ is the phonon self-energy due to the electron-phonon interaction. Migdal⁵ originally argued that $\Pi(\vec{q}, i\nu_n)$ was required for consistency and, among other things, leads to a renormalization of the phonon frequency $\omega_E \rightarrow \Omega(\vec{q})$. Since the early practice was to extract the phonon spectrum from experiment, researchers often dispensed with the calculation of $\Pi(\vec{q}, i\nu_n)$. Here it is required, since we wish to predict pending instabilities

based on the microscopic Holstein model, with no input from experiment.

Note that this notation differs slightly from that of Ref. [1], in that the bare phonon propagator differs by a factor of $2M\omega_E$ and similarly for the phonon self energy in what follows. It is clear that the unperturbed system consists of non-interacting electrons and phonons, with non-interacting propagators,

$$G_0(\vec{k}, i\omega_m) = [i\omega_m - (\epsilon_k - \mu)]^{-1} \quad (11)$$

$$D_0(\vec{q}, i\nu_m) = \frac{-2\omega_E}{(\omega_E^2 + \nu_m^2)}, \quad (12)$$

respectively.

The approximations indicated in Figs. 1a,b are [note that $\alpha^2/(2M\omega_E)$ (Ref. [1]) $\rightarrow (g\omega_E)^2$]:

$$\Sigma(\vec{k}, i\omega_m) = -\frac{(g\omega_E)^2}{N\beta} \sum_{k', m'} D(\vec{k} - \vec{k}', i\omega_m - i\omega_{m'}) G(\vec{k}', i\omega_{m'}) \quad (13)$$

$$\Pi(\vec{q}, i\nu_n) = 2 \frac{(g\omega_E)^2}{N\beta} \sum_{k, m} G(\vec{k}, i\omega_m) G(\vec{k} + \vec{q}, i\omega_m + i\nu_n). \quad (14)$$

In addition, the occupancy requirement is

$$n = \frac{2}{N\beta} \sum_{k, m} G(\vec{k}, i\omega_m) e^{i\omega_m 0^+} \quad (15)$$

which determines the chemical potential, μ . Here $\beta \equiv 1/T$, and the Matsubara sums span all integers while the wave vector is summed over the entire First Brillouin Zone, as noted below Eq. (8). There are no vertex corrections in Eqs. (13) and (14). However, Eqs.(9-10) together with Eqs. (13 - 15) form a set of *fully self-consistent* equations in two dimensional momentum and one dimensional frequency space, for the electron and phonon propagators. Alternatively, one can replace the D propagator in Eq. (13) with D_0 , and ignore Eq. (14) entirely, for the non-self-consistent approximation. We have demonstrated the need for self-consistently previously;¹ here we will carry out a more systematic investigation.

The singlet pairing (SP) and CDW susceptibilities are given by:⁶

$$\chi^{\text{SP}} = \frac{1}{N} \sum_{ij} \int_0^\beta d\tau \langle c_{i\uparrow}(\tau) c_{i\downarrow}(\tau) c_{j\downarrow}^\dagger(0) c_{j\uparrow}^\dagger(0) \rangle \quad (16)$$

$$\chi^{\text{CDW}}(\vec{q}) = \frac{1}{N} \sum_{\substack{ij \\ \sigma\sigma'}} e^{i\vec{q}\cdot(\vec{R}_i - \vec{R}_j)} \int_0^\beta d\tau [\langle n_{i\sigma}(\tau) n_{j\sigma'}(0) \rangle - \langle n_{i\sigma}(\tau) \rangle \langle n_{j\sigma'}(0) \rangle]. \quad (17)$$

In the approximations given in Fig. 1, these susceptibilities are given by

$$\chi^{\text{SP}} = \frac{1}{N\beta} \sum_{k, m} F(\vec{k}, i\omega_m) \Lambda(\vec{k}, i\omega_m) \quad \text{where} \quad F(\vec{k}, i\omega_m) = G(\vec{k}, i\omega_m) G(-\vec{k}, -i\omega_m), \quad (18)$$

and

$$\chi^{\text{CDW}}(\vec{q}) = \frac{\bar{\chi}^{\text{CDW}}(\vec{q})}{1 - \lambda_0 \bar{\chi}^{\text{CDW}}(\vec{q})} \quad \text{with} \quad \bar{\chi}^{\text{CDW}}(\vec{q}) = -\frac{1}{(g\omega_E)^2} \text{Re}[\Pi(\vec{q}, 0)] \quad (19)$$

and $\lambda_0 \equiv 2\omega_E g^2$. The function $\Lambda(\vec{k}, i\omega_m)$ is the solution of the vertex equation:

$$\Lambda(\vec{k}, i\omega_m) = 1 - \frac{(g\omega_E)^2}{N\beta} \sum_{\vec{k}' m'} F(\vec{k}', i\omega_{m'}) D(\vec{k} - \vec{k}', i\omega_m - i\omega_{m'}) \Lambda(\vec{k}', i\omega_{m'}). \quad (20)$$

Equation (20) with the “1” removed simply becomes the Eliashberg equation to determine T_c . Once again iteration is required in two dimensional momentum and one dimensional frequency space.

As emphasized in Refs. [1 and 2], the importance of including the phonon self-energy, $\Pi(\vec{q}, i\nu_n)$ in Eq. (10) is clear upon inspection of Eq. (19). We are including the CDW correlations into the one-electron Green’s function. In what follows we will call the approximation which includes $\Pi(\vec{q}, i\nu_n)$ the “renormalized Migdal-Eliashberg approximation,” and the one which omits $\Pi(\vec{q}, i\nu_n)$ the “unrenormalized Migdal-Eliashberg ap-

proximation.”

B. Matsubara Sum Speed-Ups

Some speed-up in summing the Matsubara frequencies in Eqs. (13) and (14) are as follows. We can subtract and add the summands with G and D replaced by G_0 and D_0 respectively in Eqs. (13) and (14). The Matsubara sum in the part added can then be done analytically to obtain what we will define to be $\Sigma_0(\vec{k}, i\omega_m)$ and $\Pi_0(\vec{q}, i\nu_n)$, respectively. Then we have

$$\Sigma(\vec{k}, i\omega_m) = \Sigma_0(\vec{k}, i\omega_m) - \frac{(g\omega_E)^2}{N\beta} \sum_{\vec{k}', m'} [D(\vec{k} - \vec{k}', i\omega_m - i\omega_{m'}) G(\vec{k}', i\omega_{m'}) - D_0(\vec{k} - \vec{k}', i\omega_m - i\omega_{m'}) G_0(\vec{k}', i\omega_{m'})] \quad (21)$$

$$\Pi(\vec{q}, i\nu_n) = \Pi_0(\vec{q}, i\nu_n) + 2 \frac{(g\omega_E)^2}{N\beta} \sum_{\vec{k}, m} [G(\vec{k}, i\omega_m) G(\vec{k} + \vec{q}, i\omega_m + i\nu_n) - G_0(\vec{k}, i\omega_m) G_0(\vec{k} + \vec{q}, i\omega_m + i\nu_n)]. \quad (22)$$

Similarly

$$n = n_0 + \frac{2}{N\beta} \sum_{\vec{k}, m} [G(\vec{k}, i\omega_m) - G_0(\vec{k}, i\omega_m)] e^{i\omega_m 0^+}, \quad (23)$$

where, for example, in Eq. 23) we have

$$n_0 = \frac{2}{N\beta} \sum_{\vec{k}, m} G_0(\vec{k}, i\omega_m) e^{i\omega_m 0^+} = \frac{2}{N} \sum_{\vec{k}} f(\epsilon_k - \mu), \quad (24)$$

and $f(x) \equiv 1/[\exp\{(\beta x)\} + 1]$ is the Fermi-Dirac distribu-

tion function. The Matsubara sums, which can easily be converted to positive integers only, now converge much more rapidly, and therefore fewer are required. Similar speed-ups apply to Eq. (20).

Note that

$$\Sigma_0(\vec{k}, i\omega_m) = \frac{(g\omega_E)^2}{N} \sum_{\vec{k}'} \left(\frac{1 + N(\omega_E) - f(\epsilon_{k'} - \mu)}{i\omega_m - \omega_E - (\epsilon_{k'} - \mu)} + \frac{N(\omega_E) + f(\epsilon_{k'} - \mu)}{i\omega_m + \omega_E - (\epsilon_{k'} - \mu)} \right) \quad (25)$$

and

$$\Pi_0(\vec{q}, i\nu_n) = (g\omega_E)^2 \frac{2}{N} \sum_{\vec{k}} \frac{f(\epsilon_k - \mu) - f(\epsilon_{k+q} - \mu)}{i\nu_n + \epsilon_k - \epsilon_{k+q}}, \quad (26)$$

where $N(x) \equiv 1/[\exp\{(\beta x)\} - 1]$ is the Bose-Einstein distribution function. Note that the CDW susceptibility, calculated in the non-interacting limit, is simply given by

$$\chi_0(\vec{q}, i\nu_n) = -\Pi_0(\vec{q}, i\nu_n)/(g\omega_E)^2. \quad (27)$$

C. Self-Energy Reformulation in Conjugate Variable Space

It is clear from Eqs.(13, 14) that both the electron and phonon self-energies are calculated through convolutions in reciprocal and Matsubara frequency space (although Eq. 14 has to be rewritten slightly to see this). As convolution is simply multiplication in the conjugate space, we may reformulate the self-energies accordingly. First note that the phonon self-energy can be equivalently written as:

$$\Pi(\vec{q}, i\nu_n) = 2 \frac{(g\omega_E)^2}{N\beta} \sum_{k,m} G(\vec{q} - \vec{k}, i\nu_n - i\omega_m) G^*(\vec{k}, i\omega_m), \quad (28)$$

This alternate equation for the phonon self-energy relies on the fact that $G(-\vec{k}, -i\omega_m) = G^*(\vec{k}, i\omega_m)$, where * denotes complex conjugation. Since the convolution in the above is clear, we rewrite Eq. (28) further as:

$$\Pi(\vec{q}, i\nu_n) = 2 \frac{(g\omega_E)^2}{N} \int_0^\beta d\tau \frac{1}{N} \sum_{\vec{R}_\ell} e^{-i(\vec{q} \cdot \vec{R}_\ell - \nu_n \tau)} \hat{G}(\vec{R}_\ell, \tau) \hat{G}_c(\vec{R}_\ell, \tau) \quad (29)$$

where

$$\hat{G}(\vec{R}_\ell, \tau) = \frac{1}{\beta} \sum_{\vec{k}, m} e^{i(\vec{k} \cdot \vec{R}_\ell - \omega_m \tau)} G(\vec{k}, i\omega_m) \quad (30)$$

and

$$\hat{G}_c(\vec{R}_\ell, \tau) = \frac{1}{\beta} \sum_{\vec{k}, m} e^{i(\vec{k} \cdot \vec{R}_\ell - \omega_m \tau)} G^*(\vec{k}, i\omega_m). \quad (31)$$

Similarly, the electron self-energy can be rewritten as

$$\Sigma(\vec{k}, i\omega_m) = -\frac{(g\omega_E)^2}{N} \int_0^\beta d\tau \frac{1}{N} \sum_{\vec{R}_\ell} e^{-i(\vec{k} \cdot \vec{R}_\ell - \omega_m \tau)} \hat{D}(\vec{R}_\ell, \tau) \hat{G}(\vec{R}_\ell, \tau). \quad (32)$$

where

$$\hat{D}(\vec{R}_\ell, \tau) = \frac{1}{\beta} \sum_{\vec{q}, n} e^{i(\vec{q} \cdot \vec{R}_\ell - \nu_n \tau)} D(\vec{q}, i\nu_n) \quad (33)$$

Finally, we may also rewrite the vertex equation Eq. (20) as

$$\Lambda(\vec{k}, i\omega_m) = 1 - \frac{(g\omega_E)^2}{N\beta} \int_0^\beta d\tau \frac{1}{N} \sum_{\vec{R}_\ell} e^{-i(\vec{k} \cdot \vec{R}_\ell - \omega_m \tau)} \hat{D}(\vec{R}_\ell, \tau) \hat{K}(\vec{R}_\ell, \tau) \quad (34)$$

where

$$\hat{K}(\vec{R}_\ell, \tau) = \frac{1}{\beta} \sum_{\vec{k}, m} e^{i(\vec{k} \cdot \vec{R}_\ell - \omega_m \tau)} F(\vec{k}, i\omega_m) \Lambda(\vec{k}, i\omega_m) \quad (35)$$

The above equations may easily be recast in the form of fast Fourier transforms for efficient numerical evaluation of the self-consistent equations. Further details on fast Fourier transform implementation are given in the appendix.

II. HUBBARD-HOLSTEIN MODEL

Including an on-site repulsion term to the Holstein Hamiltonian Eq. (1) leads to the Hubbard-Holstein

Hamiltonian:

$$\begin{aligned} H = & -t \sum_{\substack{i, \delta \\ \sigma}} (c_{i\sigma}^\dagger c_{i+\delta\sigma} + c_{i+\delta\sigma}^\dagger c_{i\sigma}) \\ & - g\omega_E \sum_{i,\sigma} n_{i\sigma} (a_i + a_i^\dagger) \\ & + \omega_E \sum_i a_i^\dagger a_i + U \sum_i n_{i,\uparrow} n_{i,\downarrow}. \end{aligned} \quad (36)$$

Transforming the above to reciprocal space, we get:

$$\begin{aligned} H = & \sum_{\vec{k}, \sigma} (\epsilon_{\vec{k}} - \mu) c_{\vec{k}\sigma}^\dagger c_{\vec{k}\sigma} + \omega_E \sum_{\vec{q}} a_{\vec{q}}^\dagger a_{\vec{q}} \\ & - \frac{g\omega_E}{\sqrt{N}} \sum_{\vec{k}, \vec{q}} c_{\vec{k}+\vec{q}\sigma}^\dagger c_{\vec{k}\sigma} (a_{\vec{q}} + a_{-\vec{q}}^\dagger) \\ & + \frac{U}{N} \sum_{\vec{k}, \vec{k}', \vec{q}} c_{\vec{k}'-\vec{q}\uparrow}^\dagger c_{\vec{k}+\vec{q}\downarrow}^\dagger c_{\vec{k}\downarrow} c_{\vec{k}'\uparrow}. \end{aligned} \quad (37)$$

We will study two approaches to including on-site repulsion with ME theory: the “Berger” formulation, and the “Marsiglio” formulation.

A. Hubbard-Holstein Model: Berger Formulation

Treating electron correlations on the same footing as the electron-phonon coupling, the Migdal-Eliashberg (ME) equations in diagrammatic form are shown below (according to Berger et. al.^[7]): We now translate these

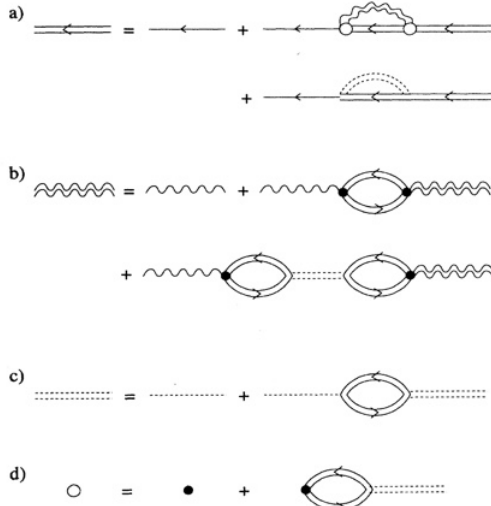


FIG. 2. The ME equations for Hubbard-Holstein model for electrons (a) and phonons (b). The single (double) solid line represents the non-interacting (interacting) electron Green’s function, the single (double) wavy line the non-interacting (interacting) phonon Green’s function. The vertex point represents the emission and absorption of a phonon. Also depicted is the screened electron-electron interaction (c) and the effective electron-phonon interaction (d). Figure and caption taken from [7].

diagrams to a set of self-consistent equations, according to Berger et.al.^[7]. We will denote ME functions for Hubbard-Holstein model analogous to their bare Holstein model counterparts with a “bar”. For example, the electron Green’s function becomes $G(\vec{k}, i\omega_m) \rightarrow \bar{G}(\vec{k}, i\omega_m)$ with the inclusion of the Hubbard U term. Note that $\bar{G}(\vec{k}, i\omega_m)|_{U=0} = G(\vec{k}, i\omega_m)$.

The Hubbard U renormalized propagators are given by

$$\bar{G}(\vec{k}, i\omega_m) = \frac{1}{i\omega_m - (\epsilon_{\vec{k}} - \mu) - \bar{\Sigma}(\vec{k}, i\omega_m)} \quad (38)$$

for electrons and

$$\bar{D}(\vec{q}, i\nu_n) = \frac{-2\omega_E}{(\omega_E^2 + \nu_n^2) + 2\omega_E \bar{\Pi}(\vec{q}, i\nu_n)} \quad (39)$$

for phonons.

To define the Hubbard U renormalized self-energies, we first define the irreducible charge susceptibility:

$$\chi(\vec{q}, i\nu_n) = \frac{1}{N\beta} \sum_{k,m} \bar{G}(\vec{q}-\vec{k}, i\nu_n - i\omega_m) \bar{G}^*(\vec{k}, i\omega_m). \quad (40)$$

The Hubbard U renormalized phonon self-energy is given by:

$$\bar{\Pi}(\vec{q}, i\nu_n) = \frac{2(g\omega_E)^2 \chi(\vec{q}, i\nu_n)}{1 - U\chi(\vec{q}, i\nu_n)}. \quad (41)$$

The Hubbard U renormalized electron self-energy is given by:

$$\bar{\Sigma}(\vec{k}, i\omega_m) = -\frac{(g\omega_E)^2}{\beta N} \sum_{\vec{k}', m'} \bar{D}_{\text{eff}}(\vec{k}-\vec{k}', i\omega_m - i\omega_{m'}) \bar{G}(\vec{k}', i\omega_{m'}), \quad (42)$$

where $\bar{D}_{\text{eff}}(\vec{q}, i\nu_n)$ is the “effective” Hubbard U renormalized phonon propagator, which is given by:

$$\bar{D}_{\text{eff}}(\vec{q}, i\nu_n) = \frac{\bar{D}(\vec{q}, i\nu_n)}{[1 - U\chi(\vec{q}, i\nu_n)]^2} + \frac{U^2}{(g\omega_E)^2} \frac{\chi(\vec{q}, i\nu_n)}{1 - [U\chi(\vec{q}, i\nu_n)]^2}. \quad (43)$$

The Hubbard U renormalized vertex equation is given by:

$$\bar{\Lambda}(\vec{k}, i\omega_m) = 1 - \frac{(g\omega_E)^2}{N\beta} \sum_{k'm'} \bar{F}(\vec{k}', i\omega_{m'}) \bar{D}_{\text{eff}}(\vec{k} - \vec{k}', i\omega_m - i\omega_{m'}) \bar{\Lambda}(\vec{k}', i\omega_{m'}) \quad (44)$$

where $\bar{F}(\vec{k}, i\omega_m) = \bar{G}(\vec{k}, i\omega_m)\bar{G}^*(\vec{k}, i\omega_m)$. The occupancy condition Eq. 23 is define analogously for $\bar{G}(\vec{k}, i\omega_m)$. The Hubbard U renormalized singlet pairing and charge density susceptibilities (χ_U^{SP} and $\chi_U^{\text{CDW}}(\vec{q})$, respectively) are defined next:

$$\chi_U^{\text{SP}} = \frac{1}{N\beta} \sum_{k,m} \bar{F}(\vec{k}, i\omega_m) \bar{\Lambda}(\vec{k}, i\omega_m), \quad (45)$$

and

$$\chi_U^{\text{CDW}}(\vec{q}) = \frac{\bar{\chi}_U^{\text{CDW}}(\vec{q})}{1 - \lambda_0 \bar{\chi}_U^{\text{CDW}}(\vec{q})} \quad \text{with} \quad \bar{\chi}_U^{\text{CDW}}(\vec{q}) = -\frac{1}{(g\omega_E)^2} \text{Re}[\bar{\Pi}(\vec{q}, 0)] \quad (46)$$

Temperature-filling phase diagrams for this model are shown below for a matrix of U and ω_E values. Note that here, we are working in units where the n.n. hopping amplitude and Boltzmann constant are set to unity $t = K_B = 1$.

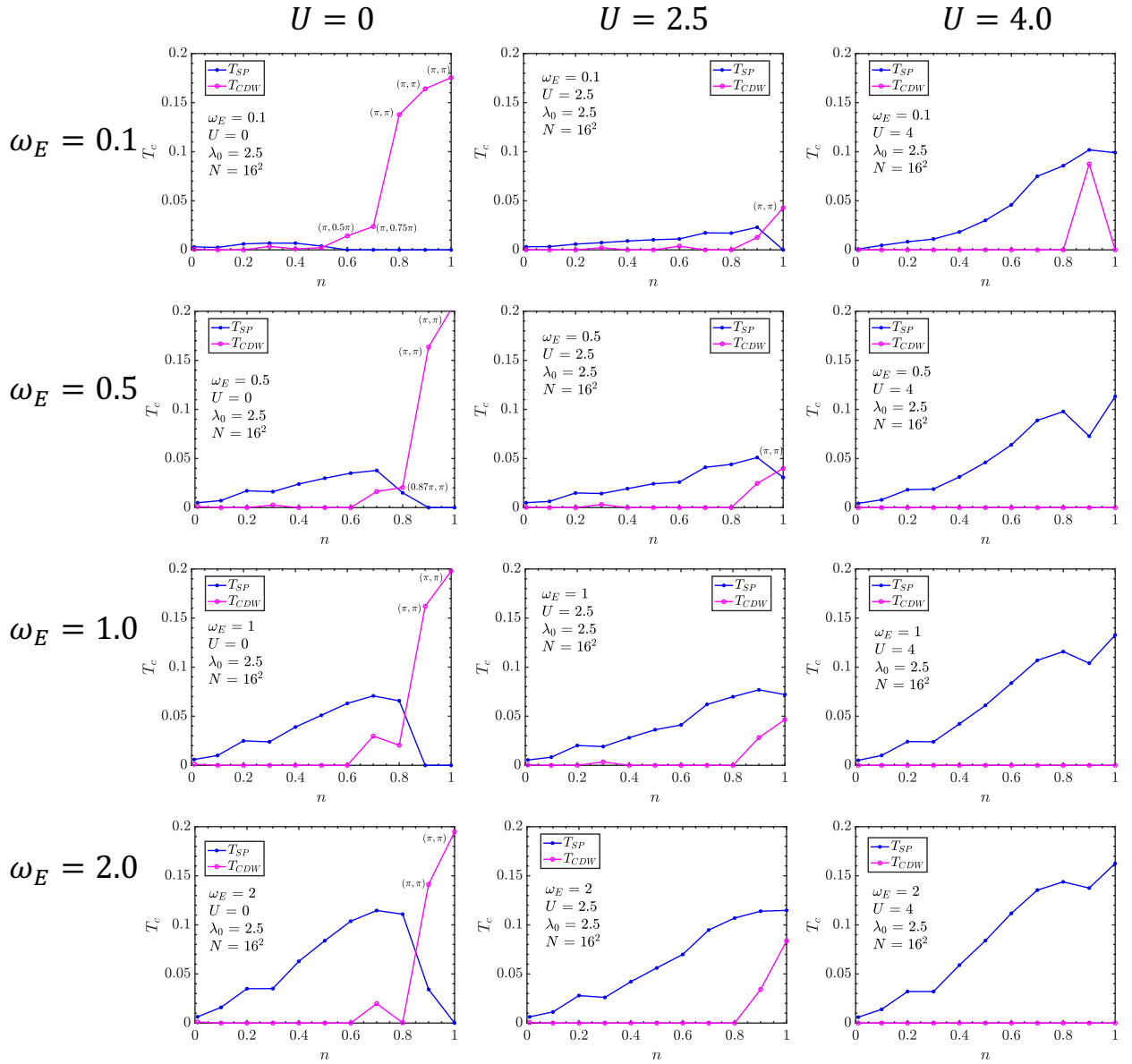


FIG. 3. Temperature-filling phase diagrams for the Hubbard-Holstein model formulated by Berger et. al. Phase diagrams are shown for $\omega_E \in \{0.1, 0.5, 1.0, 2.0\}$ and $U/t \in \{0, 2.5, 4.0\}$. Calculations are shown for a 16×16 lattice and an interaction parameter of $\lambda_0 = 2.5$. In addition, CDW critical temperatures at which $T_{CDW} > T_{SP}$ are labeled with the wave vector \vec{q} that maximizes the CDW susceptibility.

B. Hubbard-Holstein Model: Marsiglio Formulation

Marsiglio suggests a simpler approach is to be used when including U , one which does not involve collective electronic modes. The only equations adjusted are Eq. (20) and Eq. (19). With the inclusion of on-site repulsion, the vertex equation is written as:

$$\Lambda(\vec{k}, i\omega_m) = 1 - \frac{(g\omega_E)^2}{N\beta} \sum_{k'm'} F(\vec{k}', i\omega_{m'}) \left[D(\vec{k} - \vec{k}', i\omega_m - i\omega_{m'}) + \frac{U}{(g\omega_E)^2} \right] \Lambda(\vec{k}', i\omega_{m'}) \quad (47)$$

The CDW susceptibility is also modified:

$$\chi^{\text{CDW}}(\vec{q}) = \frac{\bar{\chi}^{\text{CDW}}(\vec{q})}{1 - (\lambda_0 - U)\bar{\chi}^{\text{CDW}}(\vec{q})} \quad (48)$$

Note that the above implies that the phonon propagator is no longer aware of the divergences in the CDW susceptibility. Thus, the phonon propagator may diverge even if the the CDW susceptibility does not.

Temperature-filling phase diagrams for this model are shown below for a matrix of U and ω_E values. Note that here, we are working in units where the n.n. hopping amplitude and Boltzmann constant are set to unity $t = K_B = 1$.

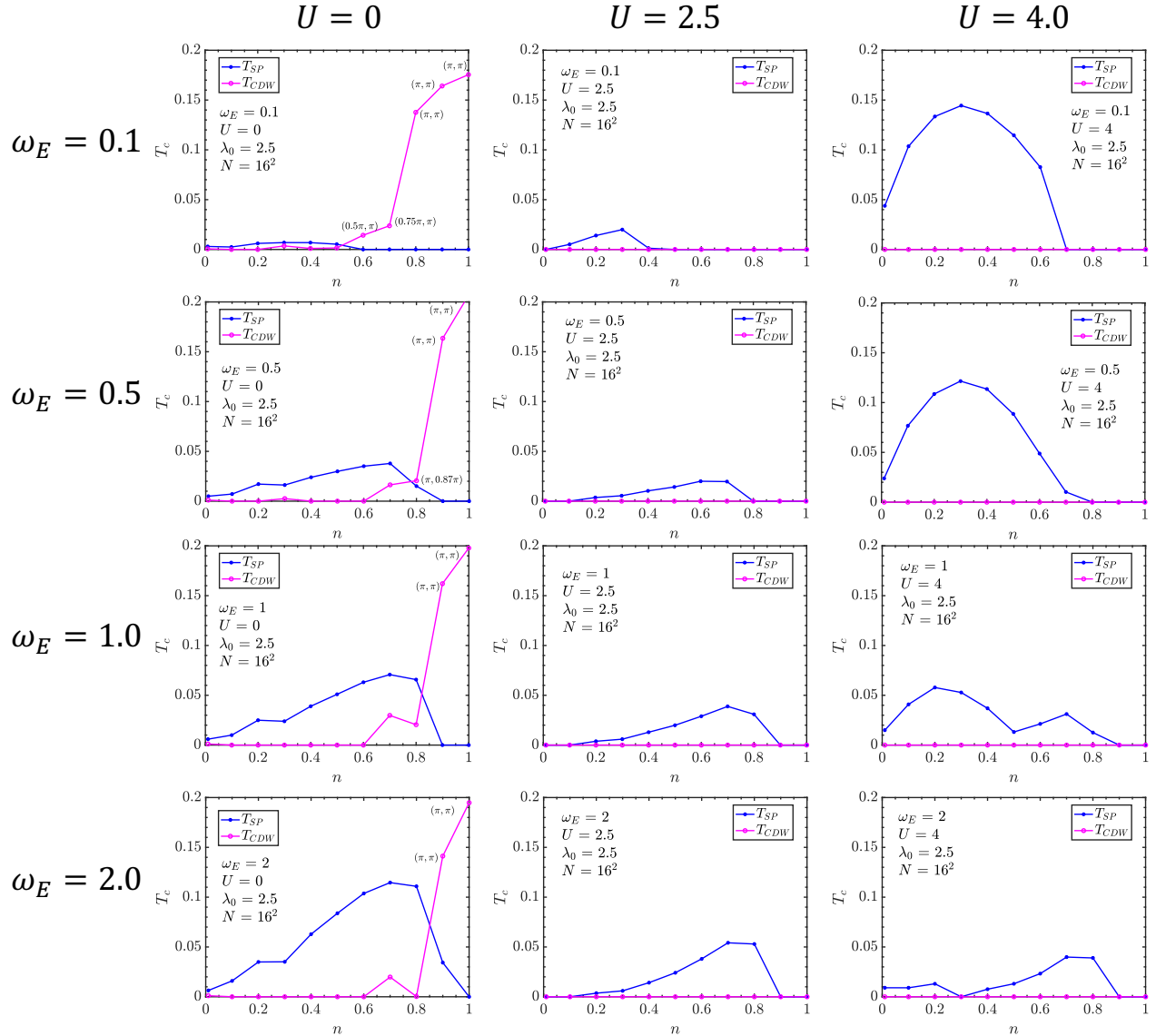


FIG. 4. Temperature-filling phase diagrams for the Hubbard-Holstein model formulated by Marsiglio. Phase diagrams are shown for $\omega_E \in \{0.1, 0.5, 1.0, 2.0\}$ and $U \in \{0, 2.5, 4.0\}$. Calculations are shown for a 16×16 lattice and an interaction parameter of $\lambda_0 = 2.5$. In addition, CDW critical temperatures at which $T_{\text{CDW}} > T_{\text{SP}}$ are labeled with the wave vector \vec{q} that maximizes the CDW susceptibility.

Appendix A: FFT Methods for Convolutions in Matsubara Space

In general, the fast Fourier transform (FFT) of a discrete vector $x_\ell \rightarrow \hat{x}_j$ of length N is defined via:

$$\hat{x}_j = \mathcal{F}\{x_\ell\}_j = \sum_{\ell=0}^{N-1} x_\ell e^{-i\frac{2\pi}{N}j\ell}. \quad (\text{A1})$$

The inverse fast Fourier transform (iFFT) is defined as

$$x_\ell = \mathcal{F}^{-1}\{\hat{x}_j\}_\ell = \frac{1}{N} \sum_{j=0}^{N-1} \hat{x}_j e^{i\frac{2\pi}{N}j\ell} \quad (\text{A2})$$

FFT algorithms are incredibly efficient, with computational complexity of order $O(N \log(N))$, where N is the size of the input data. Since our self-consistent calculations involve convolutions in wavevector and Matsubara space, we will utilize fast Fourier transforms to efficiently evaluate these equations. Since the Fourier transforms from real space to wave vector space is straightforward, we only describe the transforms from imaginary time to imaginary frequency space here.

For Fermionic Green's functions, one may transform from $i\omega_m \rightarrow \tau$ space via:

$$\hat{G}(\tau) = \frac{1}{\beta} \sum_m e^{-i\omega_m \tau} G(i\omega_m), \quad (\text{A3})$$

where $\omega_m = \frac{\pi}{\beta}(2m - 1)$, $m \in [-(M-1)/2, (M-1)/2]$, with M being the number of Matsubara frequencies used. The inverse transform $\tau \rightarrow i\omega_m$ is defined via:

$$G(i\omega_m) = \int_0^\beta d\tau e^{i\omega_m \tau} \hat{G}(\tau). \quad (\text{A4})$$

Similar transforms can be defined for Bosonic Green's functions with $i\omega_m \rightarrow i\nu_n$, where $\nu_n = \frac{2\pi}{\beta}n$, with $n \in [-(M-1)/2, (M-1)/2]$. Both Eqs. (A3) and (A4) can be recast in the form of a fast Fourier transform (FFT) and inverse fast Fourier transform (iFFT), respectively. We begin by discretizing the integral transform in Eq. (A4). More specifically, we replace the continuous variable τ with a discrete analogue: $\tau \rightarrow \tau_j = j\beta/M$, where $j = 0, 1, \dots, M-1$. This leads to the following discrete transform:

$$G(i\omega_m) = \frac{\beta}{M} \sum_{j=0}^{M-1} e^{i\omega_m j \beta/M} \hat{G}(\tau_j). \quad (\text{A5})$$

For numerical work, it is convenient to define a vector $G_m \equiv G(i\omega_{m-(M-1)/2})$. With this notation, G_0 (G_{M-1}) represents the Green's function evaluated at the negative (positive) frequency cutoff. This is consistent with the ordering used in our numerical work. We also define vector $\hat{G}_j \equiv \hat{G}(\tau_j)$ for consistency. With this notation,

we rewrite Eq. (A5) in the form of an iFFT:

$$\begin{aligned} G_m &= G(i\omega_{m-(M-1)/2}) = \frac{\beta}{M} \sum_{j=0}^{M-1} e^{i\omega_{m-(M-1)/2} \beta/M} \hat{G}_j \\ &= \frac{\beta}{M} \sum_{j=0}^{M-1} e^{i2\pi m j/M} e^{-i\pi j(M-1)/M} e^{-i\pi j/M} \hat{G}_j \\ &= \frac{\beta}{M} \sum_{j=0}^{M-1} e^{i2\pi m j/M} e^{-i\pi j} \hat{G}_j \end{aligned} \quad (\text{A6})$$

Thus, the final result is:

$$G_m = \beta \mathcal{F}^{-1} \left\{ e^{-i\pi j} \hat{G}_j \right\}_m \quad (\text{A7})$$

Similarly, the forward transform can be defined via

$$\hat{G}_j = \frac{1}{\beta} e^{i\pi j} \mathcal{F}\{G_m\}_j. \quad (\text{A8})$$

For Bosonic Green's functions, we similarly define vectors $D_n \equiv D(i\nu_{n-(M-1)/2})$ and $\hat{D}(\tau_j) \equiv \hat{D}_j$. It follows that the Bosonic transforms are given by:

$$D_n = \beta \mathcal{F}^{-1} \left\{ e^{-i\pi j(M-1)/M} \hat{D}_j \right\}_n, \quad (\text{A9})$$

and

$$\hat{D}_j = \frac{1}{\beta} e^{i\pi j(M-1)/M} \mathcal{F}\{D_n\}_j \quad (\text{A10})$$

Using Eqs. (A7 - A10), we may evaluate the Matsubara space convolutions in Eqs. (13), (14), and (20). The phonon self-energy can be rewritten in the form of a standard convolution as follows:

$$\begin{aligned} \Pi(i\nu_n) &= 2 \frac{(g\omega_E)^2}{N\beta} \sum_m G(i\nu_n + i\omega_m) G(i\omega_m) \\ &= 2 \frac{(g\omega_E)^2}{N\beta} \sum_{-m} G(i\nu_n - i\omega_m) G(-i\omega_m) \\ &= 2 \frac{(g\omega_E)^2}{N\beta} \sum_m G(i\nu_n - i\omega_m) G^*(i\omega_m) \end{aligned} \quad (\text{A11})$$

where $G^*(i\omega_m)$ denotes the complex conjugate. Note that we are only considering the imaginary frequency dependence of the phonon self-energy. Switching to the notation we've adopted for numerical work, the above is equivalent to:

$$\Pi_n = 2 \frac{(g\omega_E)^2}{N\beta} \sum_{m=0}^{M-1} G_{n-m} G_m^*. \quad (\text{A12})$$

Finally, we rewrite the above in terms of FFTs as follows:

$$\Pi_n = 2 \frac{(g\omega_E)^2}{N\beta} \mathcal{F}^{-1} \left\{ e^{-i\pi j(M-1)/M} \mathcal{F}\{G_m\}_j \mathcal{F}\{G_m^*\}_j \right\}_n. \quad (\text{A13})$$

Essentially, we apply a forward fermionic Fourier transforms to both G_m and its complex conjugate, multiply the results, and then apply an inverse bosonic Fourier transform to the product. The electron self-energy can be handled similarly. We find:

$$\Sigma_m = -\frac{(g\omega_E)^2}{N\beta} \mathcal{F}^{-1}\{e^{i\pi j(M-1)/M} \mathcal{F}\{D_n\}_j \mathcal{F}\{G_m\}_j\}_m \quad (\text{A14})$$

Here, we apply a forward fermionic Fourier transform to G_m and a forward bosonic Fourier transform to D_n , multiply the results, and then apply an inverse fermionic Fourier transform to the product.

The vertex equation can be rewritten similarly:

$$\Lambda_m = 1 - \frac{(g\omega_E)^2}{N\beta} \mathcal{F}^{-1}\{e^{i\pi j(M-1)/M} \mathcal{F}\{D_n\}_j \mathcal{F}\{F_m \Lambda_m\}_j\}_m \quad (\text{A15})$$

Appendix B: Anderson Mixing

The evaluation of the set of self-consistent equations formed by Eqs. (9), (10), (13), and (14) is performed by making an initial guess for the electron self-energy and iteratively improving our guess until convergence is achieved within a preset tolerance. The most simple way to improve our guess is to set the new trial electron self-energy as a linear mixture of the calculated and old trial electron self-energy. Mathematically, the ℓ^{th} guess for the electron self-energy is calculated via:

$$\Sigma_{\text{trial}}^{(\ell)} = \Sigma_{\text{trial}}^{(\ell-1)} + b \left(\Sigma_{\text{calc}}^{(\ell-1)} - \Sigma_{\text{trial}}^{(\ell-1)} \right), \quad (\text{B1})$$

where b is a damping factor. The value of b chosen may be constant or iteratively improved as well. However, an optimal value of b is usually determined empirically.

Anderson mixing generalizes linear mixing to include an optimal linear combination of the previous M guesses. This inclusion of memory accelerates the rate of convergence.

For ease of explanation, we introduce new notation. Consider an input vector $|x\rangle$ and output vector $|y\rangle$ that are to be converged to one another within a tolerance ε

such that $\max(|y\rangle - |x\rangle) < \varepsilon$. Let the ℓ^{th} iteration of $|x\rangle$ be defined as $|x_\ell\rangle$, and similarly so for $|y\rangle$. We define the residual vector of the ℓ th iteration as

$$|R_\ell\rangle = |y_\ell\rangle - |x_\ell\rangle \quad (\text{B2})$$

Linear mixing prescribes that the next guess for the input vector be

$$|x_{\ell+1}\rangle = |x_\ell\rangle + b|R_\ell\rangle \quad (\text{B3})$$

for some damping factor b . Anderson mixing prescribes that the next guess is for the input vector is instead given by:

$$|x_{\ell+1}\rangle = |\bar{x}_\ell\rangle + b|\bar{R}_\ell\rangle, \quad (\text{B4})$$

where

$$|\bar{x}_\ell\rangle = |x_\ell\rangle - \sum_{j=1}^M C_j^\ell |\Delta x_{\ell-j}\rangle, \quad |\Delta x_{\ell-j}\rangle \equiv |x_\ell\rangle - |x_{\ell-j}\rangle$$

$$(\text{B5})$$

$$|\bar{R}_\ell\rangle = |R_\ell\rangle - \sum_{j=1}^M C_j^\ell |\Delta R_{\ell-j}\rangle, \quad |\Delta R_{\ell-j}\rangle \equiv |R_\ell\rangle - |R_{\ell-j}\rangle, \quad (\text{B6})$$

with $M = 1, 2, 3, \dots, \ell-1$. The vector $|\bar{y}_\ell\rangle$ is defined similarly. These equations essentially mix the most recent guess for $|x\rangle$ with its incremental differences with the M previous guesses. The coefficients C_j^ℓ are chosen such that the square norm of $|\bar{R}_\ell\rangle$ is minimized. Thus, the optimal coefficients are calculated by solving the following matrix equation:

$$\sum_{j=1}^M \langle \Delta R_{\ell-i} | \Delta R_{\ell-j} \rangle C_j^\ell = \langle \Delta R_{\ell-i} | R_\ell \rangle \quad i = 1, 2, 3, \dots, M. \quad (\text{B7})$$

With Anderson mixing, we found that using a value of $b = 1$ and $M \in [3, 5]$ is sufficient to accelerate convergence.

¹ F. Marsiglio, *Physica C: Superconductivity and its Applications* **162-164**, 1453 (1989).

² F. Marsiglio, arXiv preprint arXiv:2101.12084 (1991).

³ R. T. Scalettar, N. E. Bickers, and D. J. Scalapino, *Phys. Rev. B* **40**, 197 (1989).

⁴ G. Levine and W. P. Su, *Phys. Rev. B* **42**, 4143 (1990).

⁵ A. Migdal, *Sov. Phys. JETP* **7**, 996 (1958).

⁶ J. E. Hirsch and D. J. Scalapino, *Phys. Rev. B* **32**, 117 (1985).

⁷ E. Berger, P. Valášek, and W. von der Linden, *Phys. Rev. B* **52**, 4806 (1995).